



Catalysts for oxygen reduction from heat-treated carbon-supported iron phenantroline complexes

M. BRON*, S. FIECHTER, M. HILGENDORFF and P. BOGDANOFF

Hahn-Meitner-Institut Berlin, Department Solar Energetics, SE5, Glienicker Strasse 100, D-14109 Berlin, Germany (*author for correspondence, present address: TU Darmstadt, Institute of Chemical Technology, Petersenstrasse 20, D-64287 Darmstadt, Germany, fax: + 49 6151 164788, e-mail: Bron@ct.chemie.tu-darmstadt.de)

Received 2 March 2001; accepted in revised form 20 November 2001

Key words: carbon, catalyst, iron, oxygen reduction, PEM-FC

Abstract

Oxygen reduction catalysts were prepared by heat treatment of carbon supported iron phenantroline complexes in Ar or NH₃. The optimum carbon black loading with iron was found to be 2%, the optimum heat treatment temperature was about 800 °C. X-ray diffractograms and TEM showed the occurrence of crystalline species at higher catalyst loadings; however, these species seem not to contribute significantly to the catalytic activity. From the slope of the Koutecky–Levich plot, an average number of 3.7 electrons transferred per oxygen molecule was calculated, which is consistent with RRDE data. A Tafel slope of about 120 mV (decade)⁻¹ indicates that the first electron transfer is rate determining.

1. Introduction

Heat-treated macrocyclic transition metal complexes, such as porphyrins or phthalocyanines ('N₄-chelates'), with Fe and Co as the central atom have been investigated regarding their properties as oxygen reduction catalysts as well as their physico-chemical properties [e.g., 1–19]. Their enhanced stability – compared to that of nonheat-treated complexes – and their reasonable activity make them suitable alternatives for platinum as cathode catalysts in polymer electrolyte membrane fuel cells. However, long term stability of these catalysts is only observed when they are heat treated at temperatures above 700 °C [4, 6, 8–11]. It is now generally believed that the N₄Me moiety, which is considered to be the active centre at lower heat-treatment temperatures (500–700 °C) [3, 6, 11, 18, 19], is largely destroyed and a new type of active centre is formed. The idea occurred that it is possible to generate such catalysts when other precursors than macrocyclic complexes are heat treated. Indeed, investigations using N-containing polymers [20–25], N-containing precursors like acetonitrile [26–29] or pyrrole and derivatives [20], or others [25] or even a carbon carrier modified with nitrogen [30], or a carbon carrier prepared during catalyst synthesis from a molecular precursor (PTCDA) [31, 32] together with transition metal salts (mainly Fe and Co) and heat treating them at temperatures above 700 °C, led to catalysts, which showed oxygen reduction at reasonably low overpotentials. Although the catalytically active centre of such catalysts is still a subject of

ongoing research, it appears that it consists of a transition metal ion, which is coordinated to pyridine-type nitrogen atoms in a way which may be similar to that of the macrocyclic complex. Therefore, we tried to produce oxygen reduction catalysts using a nonmacrocyclic precursor, in which the transition metal is already coordinated to nitrogen in a pyridine-type environment. The iron phenantroline complex is such a system. Additional motivation for this investigation came from a recent study of Levèvre et al. [33], which identified via ToF-SIMS the ion FeN₂C₄⁺ as a signature of the active centre.

This study reports electrochemical, XRD and TEM characterization of iron phenantroline complexes adsorbed onto carbon black and heat treated at temperatures above 600 °C in different atmospheres.

2. Experimental details

2.1. Catalyst preparation

The catalyst precursors were prepared by impregnating a commercial carbon black (Vulcan XC72, Cabot) with an aqueous solution of an iron(II)-(1,10)-phenantroline-complex ([Fe(C₁₂H₈N₂)₃]²⁺, referred to in the following as Fe(phen)₃). Carbon black was mixed with an aqueous solution containing an appropriate amount of Fe(phen)₃. The amount of complex in the solution was varied in order to give catalysts with different metal loading of the carbon black. Catalysts, with metal loadings from 0.5%

to 10% related to the amount of iron and carbon black used in the synthesis, were prepared. After thorough stirring and sonicating for at least 30 min, the resulting paste was dried in an oven at 90 °C overnight. The catalyst precursor was then ground to a fine powder. The precursor was then subjected to a heat treatment step: 100 mg of the precursor were filled in a quartz tube, the closed side of which was placed in an oven, and the open end connected to either a vacuum system or to a gas supply system. The quartz tube loaded with catalyst was first evacuated and then refilled with either Ar or NH₃ to a pressure of 500 mbar. The oven was heated to the desired temperature (650–1000 °C, see Section 3 for details) and left for 2 h. Afterwards, the oven was removed, and the catalyst was allowed to cool in the respective atmosphere (Ar or NH₃). Heat-treatment steps under continuous gas flow were avoided to minimize evaporation of phenantroline, which always occurred and could be seen as a precipitate at the walls of the quartz tube. Due to this evaporation the nominal catalyst loading is related to carbon black and iron only. However, the real amount of metal in the catalyst is somewhat lower, since the precursor phenantroline also takes part in the catalyst formation. For example, the amount of metal in a catalyst heat treated in Ar, which nominally contained 1.4% Fe related to carbon black, has been determined to be 1.14% using neutron activation analysis.

2.2. Electrochemical characterization

The electrochemical characterization of the catalysts was carried out via cyclic voltammetry and rotating disc electrode (RDE) measurements. The electrodes for the RDE measurements consisted of glassy carbon rods (dia. 3 mm) which were embedded in a Teflon holder. The glassy carbon (GC) rods were covered with a mixture of the catalyst powder and Nafion® in the following way: 1 mg of catalyst was suspended in 200 µl of a 50–50 water–ethanol mixture containing 0.15% Nafion®. Twice 2.5 µl of this suspension were dropped onto the GC rod. After evaporation of the solvent and drying in an oven at 90 °C, a homogeneous, thin catalyst film formed on the electrode surface. In a series of experiments (not presented here) it has been confirmed that diffusion limitations in the electrode film can be neglected.

A one-compartment glass cell and a platinum wire counter electrode, as well as a Hg|Hg₂SO₄|0.5 M H₂SO₄ reference electrode (+0.65 V vs SHE) were used. All potentials in this paper are reported with respect to the standard hydrogen electrode.

After immersion into nitrogen-purged 0.5 M H₂SO₄, the electrode was exposed to cyclic voltammetry between 0 and 0.74 V for 10 min. A cyclic voltammogram (CV) was recorded. The electrolyte solution was then saturated with oxygen for 10 min while cycling the electrode between 0 and 0.74 V. A CV was recorded and subsequent the RDE-measurements were carried out.

2.3. XRD and TEM measurements

XRD analysis of the catalysts was carried out employing a Siemens diffractometer D500/5000 in Bragg–Brentano θ – 2θ geometry using CuK α -radiation. As sample holder a (1 0 0)-oriented silicon disc was used. The diffractograms measured were identified using the JCPDS data bank.

TEM-measurements were carried out on a Philips CM 12 equipped with a super twin lens and a slow scan CCD camera. The acceleration voltage was 120 kV.

3. Results and discussion

Catalysts prepared with varying metal loading and heat treatment procedures were examined in RDE-experiments. Typical polarization curves for oxygen reduction at a catalyst containing 1.4% Fe can be seen in Figure 1 for several electrode rotation rates. No defined diffusion plateau is reached, however, the curves are well separated and exhibit the typical S-shape for RDE experiments. Analysis of the RDE curves was carried out using the Koutecky–Levich equation:

$$\frac{1}{j} = \frac{1}{B\omega^{1/2}} + \frac{1}{j_k} \quad (1)$$

where B is the Levich constant, ω the electrode rotation rate, and j_k and j are kinetic current density and the total current density at a given electrode potential, respectively.

A plot of $1/j$ against $\omega^{-1/2}$ (Koutecky–Levich plot) can be used to determine the value of B . Figure 2 shows the Koutecky–Levich plot for the RDE curves from Figure 1 for various potentials. Parallel straight lines indicate a reaction order of one with respect to oxygen. The number of electrons transferred per oxygen molecule can be obtained from the Levich constant B (Equation 1) via the following equation:

$$B = 0.2 n F c_0 D^{2/3} \nu^{-1/6} \quad (2)$$

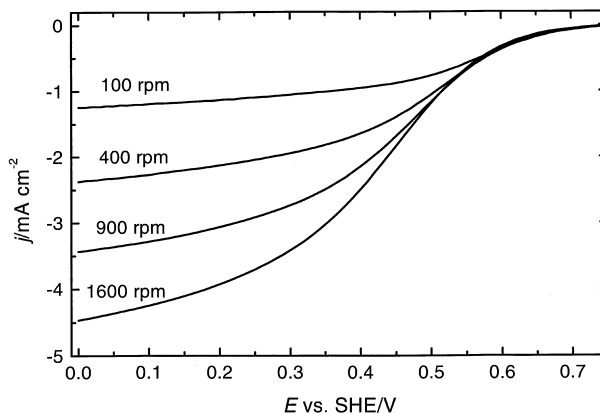


Fig. 1. RDE curves for oxygen reduction at a catalyst containing 1.4% Fe as Fe(phen)₃, supported onto carbon and heat treated in Ar at 900 °C for 2 h. Rotation rates as indicated, scan rate 5 mV s⁻¹. Oxygen saturated 0.5 M H₂SO₄.

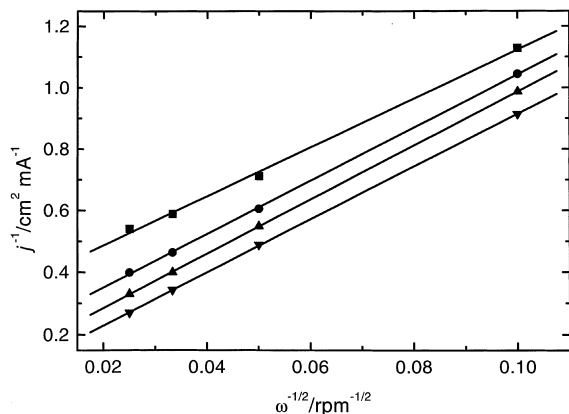


Fig. 2. Koutecky–Levich plots for oxygen reduction for different potentials as obtained from RDE curves of Figure 1. Key: (■) 0.45, (●) 0.40, (▲) 0.35 and (▼) 0.25 V vs SHE.

where n is the number of electrons, F (faradaic constant) = $96\,486.7\text{ C mol}^{-1}$, [34], c_0 (bulk concentration of oxygen) = $1.13 \times 10^{-6}\text{ mol cm}^{-3}$ [35], D (diffusion coefficient for oxygen) = $1.8 \times 10^{-5}\text{ cm}^2\text{ s}^{-1}$ [35], ν (viscosity of electrolyte) = $10.78 \times 10^{-2}\text{ cm}^2\text{ s}^{-1}$ [36]. The values are given for $0.5\text{ M H}_2\text{SO}_4$.

Using these values, a number of 3.7 electrons per oxygen molecule was calculated from the slope $1/B$ of the Koutecky–Levich plot, indicating almost complete reduction to water and a low H_2O_2 production during oxygen reduction. Preliminary RRDE results indicate an amount of H_2O_2 production of 12% at more positive potentials, decreasing to 6% at more negative potentials. This would correspond to a number of 3.76 or 3.88 electrons, respectively, under the simplified assumption of a parallel reaction of oxygen to water or hydrogen peroxide. Bouwkamps–Wijnoltz et al. [17] concluded from a detailed RRDE study on heat-treated FeTTP–Cl, that a four-electron process at more positive and a two-electron reduction at more negative potentials occurs, whereas the last one is overcompensated by a high rate of H_2O_2 reduction. The same may apply in the case of this catalyst, leading to the mentioned decreases of H_2O_2 production. Preliminary experiments on H_2O_2 reduction at a 1.4% $\text{Fe}(\text{phen})_3/\text{V}$ catalyst heat treated at $900\text{ }^\circ\text{C}$ in Ar indeed showed a high rate of H_2O_2 reduction at more negative potentials.

The determination of B from the slope of the Levich–Koutecky plot, as explained above, in turn allows calculation of the kinetic current j_k , which then can be displayed in semi-logarithmic plots against the potential E , the so called Tafel plots.

Figure 3 shows Tafel plots of the catalytic activity for oxygen reduction for a catalyst containing 1.4% Fe. It can be seen that the catalytic activity of a $\text{Fe}(\text{phen})_3/\text{V}$ catalyst heat treated in NH_3 (■) is essentially higher than the one of the same catalyst heat treated in Ar (●). Comparing the experiments of heat treatment in Ar and NH_3 , respectively, it appears, that the nitrogen, which is necessary for the formation of the active part of the catalyst [26], mainly comes from NH_3 . However, comparison of experiments

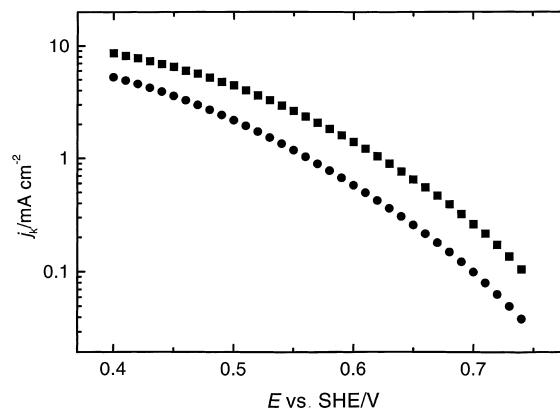


Fig. 3. Tafel plots for oxygen reduction at catalyst containing nominally 1.4% Fe as $\text{Fe}(\text{phen})_3$, supported onto carbon and heat treated in different atmospheres: NH_3 , $800\text{ }^\circ\text{C}$ (■) or Ar (●), $800\text{ }^\circ\text{C}$. Data obtained from RDE measurements in oxygen saturated $0.5\text{ M H}_2\text{SO}_4$.

of $\text{Fe}(\text{phen})_3$ with results of experiments not presented here, in which carbon supported precursors from FeSO_4 , $\text{Fe}(\text{CN})_6^{4-}$ or from iron bipyridyl complexes were heat treated in Ar, strongly indicate, that the use of phenanthroline complex as precursor enhances the activity of the catalyst, indicating that phenanthroline takes part in the formation of the active centre.

Reference trials using a carbon black impregnated with phenanthroline without iron clearly indicated, that the observed activity towards oxygen reduction is due to the heat treated $\text{Fe}(\text{phen})_3$ -complex and not due to either part of it.

To determine the optimum iron loading, catalysts with different loadings were prepared and heat treated in argon atmosphere at $900\text{ }^\circ\text{C}$. The results are displayed in Figure 4, where the kinetic current density at 0.6 V vs SHE (as a measure for oxygen reduction activity), taken from RDE experiments, is given as a function of catalyst loading. It can be seen that an optimum in activity is reached when the catalyst contains nominally about 2 wt% iron. At higher loadings, the activity decreases. This may be due to the formation of crystalline particles (see below), which do not contribute to the oxygen

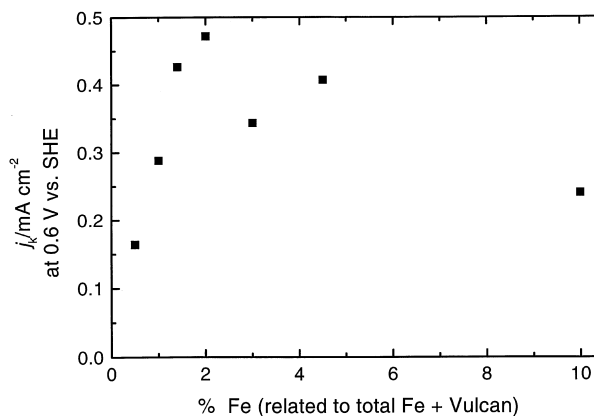


Fig. 4. Dependence of the oxygen reduction activity from the metal loading of the catalyst. Activity given as kinetic current density at 0.6 V vs SHE , as obtained from RDE measurements. All catalysts heat treated in Ar at $900\text{ }^\circ\text{C}$ for 2 h.

reduction activity [26, 27]. In other publications on similar catalysts, optimum iron loadings have been found to be much lower (below 1%; e.g., [30, 32]). However, the optimum value for iron loading also seems to depend on the precursor used in the preparation of the catalyst [33]. Using Cl-FeTMPP, Lefèvre et al. also found 2% to be the optimum value [33]. The differences have been attributed to different degree of dispersion of the catalyst precursor. In fuel cell-tests, these catalysts showed a better performance than those prepared from iron acetate, probably indicating the formation of a higher number of active sites. A better precursor distribution therefore should enhance the optimum amount of iron and enhance catalytic activity.

Formation of crystalline particles at higher metal loadings is also evidenced by XRD and TEM. Figure 5 shows X-ray diffractograms of catalysts heat treated in Ar at 900 °C. Broad lines with maxima at $2\theta = 25^\circ$ and 44° were observed, which are attributed to diffraction signals of the supporting carbon, the signal at $2\theta = 33.1^\circ$ is due to the sample holder. However, the line at $2\theta = 44^\circ$ is superimposed by another more narrow line. This line can be attributed to α -Fe and/or iron-carbon species Fe_xC_y ('martensite'). The other lines in Figure 5, together with the one at $2\theta = 44^\circ$, can be attributed to Fe_{1-x}S ('pyrrhothite'). This species obviously forms via reduction of sulfate, which is present in the catalyst as anion of the precursor salt.

The increase in signals of crystalline particles seen in Figure 5 with decrease of activity found in this study supports the view that these particles do not contribute significantly to the catalytic activity. TEM images also show the occurrence of crystalline particles. In Figure 6, such a particle can be seen. It seems to be surrounded by a layer of graphitic-type carbon. The formation of crystalline particles mostly encapsulated by graphitic carbon has also been found in other studies on similar catalysts [26, 27]. These particles do not contribute to the catalytic activity.

In another series of experiments, the optimum heat treatment temperature has been identified. In Figure 7,

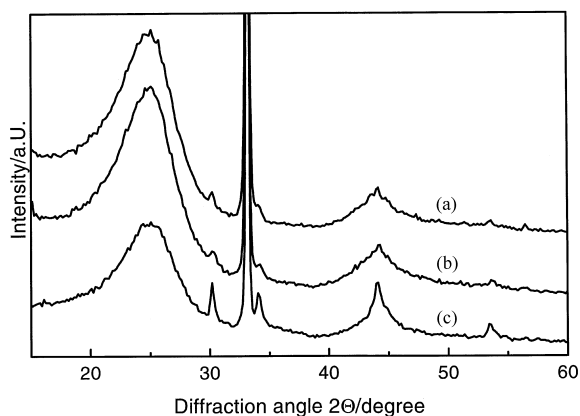


Fig. 5. X-ray diffractograms for catalysts with different iron loadings, as indicated. All catalysts heat treated in Ar at 900 °C for 2 h. Key: (a) 1.4% Fe, (b) 3.0% Fe and (c) 10.0% Fe.

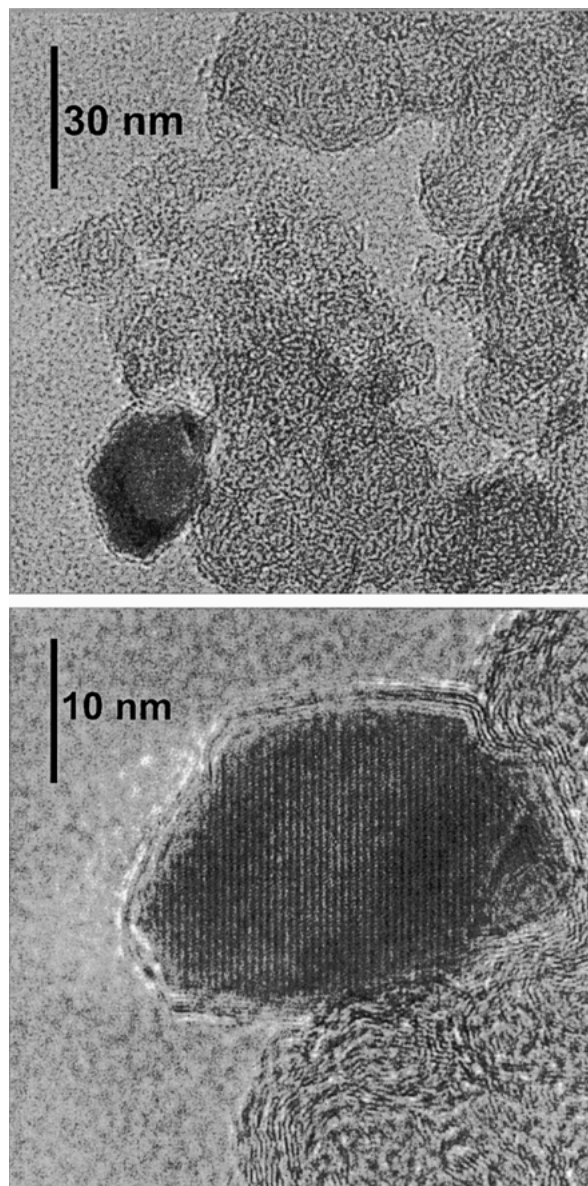


Fig. 6. TEM images of a catalyst containing 1% Fe from $\text{Fe}(\text{phen})_3$, heat treated in Ar at 900 °C for 2 h.

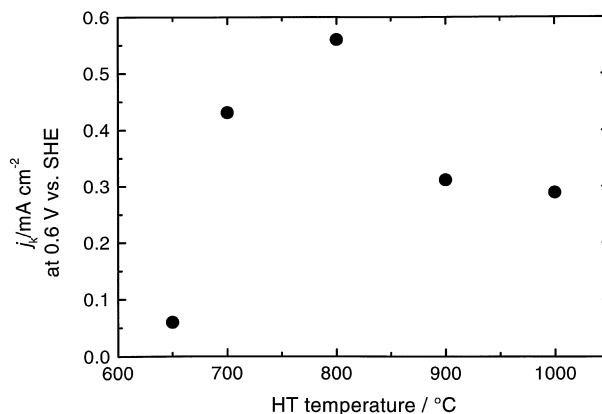


Fig. 7. Dependence of the oxygen reduction activity from the heat treatment temperature for catalysts heat treated in Ar. Activity given as kinetic current density at 0.6 V vs SHE, as obtained from RDE measurements in oxygen saturated 0.5 M H_2SO_4 .

Table 1. Peak potentials (E_p), overvoltages (η), kinetic currents (j_k) and Tafel slopes (α) of selected catalysts

Catalyst loading /%	Heat treatment /°C	α /mV dec ⁻¹	η vs 1.229 V /mV	j_k at 0.6 V vs SHE /mA cm ⁻²	Peak potential, E_p /V vs SHE
1	Ar 900	117.7	450	0.287	395
2	Ar 900	117.0	417	0.472	450
1	NH ₃ 700	121.0	423	0.431	460
1	NH ₃ 800	119.0	405	0.56	500
2	NH ₃ 800	109.9	398	1.22	480

catalytic activities of a catalyst containing 1% Fe, heat treated in NH₃ at different temperatures, are given as current densities at 0.6 V vs SHE. An optimum heat treatment temperature of about 800 °C is found. Using Ar atmosphere in the heat treatment step, the optimum activity is somewhat higher. Similar values have been found in other studies [33]. The differences between Ar and NH₃ may be explained by the reaction of NH₃ with the supporting carbon. This reaction can contribute to the formation of active centres, on the other hand, when the temperature is too high, etching of carbon also occurs, which may lead to the distortion of active parts.

Peak potentials (E_p), overvoltages (η), kinetic currents (j_k) and Tafel slopes (α) of selected catalysts are summarized in Table 1. Peak potentials have been obtained via cyclic voltammetry using the same experimental conditions as for the RDE measurements but a scan rate of 50 mV s⁻¹. As can be seen from Figure 3, no extended linear region can be found in the Tafel plots. Therefore, the slope has been estimated in the region of the beginning oxygen reduction, that is, at 0.74 to 0.64 V (Figure 1). The variations in α may be explained by traces of Fe^{2+/3+}, which are still present in the catalyst and overlap with the oxygen reduction current; however, a value of about 120 mV (decade)⁻¹ is generally attributed to a first electron transfer as rate determining step. The Tafel slope is nearly independent of the heat treatment temperature and the atmosphere employed; however, the overvoltages are generally lower when using NH₃.

No conclusion can be drawn from the data presented about the structure of the active centre. According to the literature, it consists of iron centres within a carbon–nitrogen network. Such centres must be capable of providing four electrons for a four-electron reduction of oxygen to water, as suggested by the low H₂O₂ formation. Direct four-electron reduction would require the formation of clusters, which may act as electron reservoirs, or delocalized π -electron systems, which are able of delivering necessary electrons on the timescale of the experiment. However, as suggested by the preliminary RRDE data, it may be that we are dealing with a double two-electron reduction.

From the kinetic current densities at 0.6 V, it can be seen that the most active catalyst in this study was a 2% Fe(phen)₃/V catalyst heat treated in 800 °C in NH₃. The activity of these catalysts is lower than that of heat treated macrocyclic transition metal complexes but higher than that of heat treated nitrogen-containing

polymers with transition metals, which are also under investigation in our laboratories. However, preliminary results indicate that improvement of the catalyst is possible. The use of a different carbon support, as well as a more sophisticated catalyst preparation and heat treatment procedure, will be investigated in the near future.

4. Conclusion

Oxygen reduction catalysts can be obtained on the basis of heat-treated, carbon-supported iron phenanthroline complexes. An optimum value for the metal loading of about 2% has been found. The optimum heat treatment temperature depends on the atmosphere in which the catalyst is heat treated and is about 800 °C in NH₃. A Tafel slope of about 120 mV (decade)⁻¹ at lower overvoltages indicates that the first electron transfer during oxygen reduction is rate determining. The H₂O₂ production of the catalysts is low. The activity of the catalysts is still inferior to that of heat treated macrocyclic transition metal complexes but further improvement may be possible.

Acknowledgements

The help of U. Bloeck and M. Giersig from HMI Berlin, in performing TEM measurements, is gratefully acknowledged. Financial support was obtained by the BMBF under contract 0327067 B.

References

1. D. Scherson, A.A. Tanaka, S.L. Gupta, D. Tyrk, C. Fierro, R. Holze and E.B. Yeager, *Electrochim. Acta* **31** (1986) 1247.
2. K. Wiesener, *Electrochim. Acta* **31** (1986) 1073.
3. J.A.R. van Veen, H.A. Colijn and J.F. van Baar, *Electrochim. Acta* **33** (1988) 801.
4. G. Lalande, R. Côté, G. Tamizhmani, D. Guay, J.P. Dodelet, L. Dignard-Bailey, L.T. Weng and P. Bertrand, *Electrochim. Acta* **40** (1995) 2635.
5. A. Widelöv, *Electrochim. Acta* **38** (1993) 2493.
6. G. Lalande, G. Faubert, R. Côté, D. Guay, J.P. Dodelet, L.T. Weng and P. Bertrand, *J. Power Sources* **61** (1996) 227.
7. S.L. Gojkovic, S. Gupta and R.F. Savinell, *J. Electrochem. Soc.* **145** (1998) 3493.
8. S.L. Gojkovic, S. Gupta and R.F. Savinell, *J. Electroanal. Chem.* **462** (1999) 63.
9. S.L. Gojkovic, S. Gupta and R.F. Savinell, *Electrochim. Acta* **45** (1999) 889.

10. E. Claude, T. Addou, J-M. Latour and P. Aldebert, *J. Appl. Electrochem.* **28** (1998) 57.
11. G. Faubert, G. Lalande, R. Côté, D. Guay, J.P. Dodelet, L.T. Weng, P. Bertrand and G. Dénès, *Electrochim. Acta* **41** (1996) 1689.
12. R. Jiang and D. Chu, *J. Electrochem. Soc.* **147** (2000) 4605.
13. G.Q. Sun, J.T. Wang and R.F. Savinell, *J. Appl. Electrochem.* **28** (1998) 1087.
14. I.T. Bae, D.A. Tyrk and D.A. Scherson, *J. Phys. Chem. B* **102** (1998) 4114.
15. G. Faubert, R. Côté, D. Guay, J.P. Dodelet, G. Dénès and P. Bertrand, *Electrochim. Acta* **43** (1998) 341.
16. M.C. Martins Alves, J.P. Dodelet, D. Guay, M. Ladouceur and G. Tourillon, *J. Phys. Chem.* **96** (1992) 10898.
17. A.L. Bouwkamp-Wijnoltz, W. Visscher and J.A.R. van Veen, *Electrochim. Acta* **43** (1998) 3141.
18. B. van Wingerden, J.A.R. van Veen and C.T.J. Mensch, *J. Chem. Soc. Faraday Trans. I* **84** (1988) 65.
19. R.W. Joyner, J.A.R. van Veen and W.M.H. Sachtler, *J. Chem. Soc. Faraday Trans. I* **78** (1982) 1021.
20. A.L. Bouwkamp-Wijnoltz, W. Visscher, J.A.R. van Veen and S.C. Tang, *Electrochim. Acta* **45** (1999) 379.
21. C. Fabjan, G. Frithum and H. Hartl, *Ber. Bunsenges. Phys. Chem.* **94** (1990) 937.
22. D. Ohms, S. Herzog, R. Franke, V. Neumann, K. Wiesener, S. Gamburgcev, A. Kaisheva and I. Iliev, *J. Power Sources* **38** (1992) 327.
23. S. Gupta, D. Tyrk, I. Bae, W. Aldred and E. Yeager, *J. Appl. Electrochem.* **19** (1989) 19.
24. W. Seeliger and A. Hamnett, *Electrochim. Acta* **37** (1992) 763.
25. R. Côté, G. Lalande, D. Guay and J.P. Dodelet, *J. Electrochem. Soc.* **145** (1998) 2411.
26. G. Lalande, R. Côté, D. Guay, J.P. Dodelet, L.T. Weng and P. Bertrand, *Electrochim. Acta* **42** (1997) 1379.
27. G. Faubert, R. Côté, D. Guay, J.P. Dodelet, G. Dénès, C. Poleunis and P. Bertrand, *Electrochim. Acta* **43** (1998) 1969.
28. G. Wei, J.S. Wainright and R.F. Savinell, *J. New Mat. Electrochem. Systems* **3** (2000) 121.
29. J. Fournier, G. Lalande, R. Côté, D. Guay and J.P. Dodelet, *J. Electrochem. Soc.* **144** (1997) 218.
30. H. Wang, R. Côté, G. Faubert, D. Guay and J.P. Dodelet, *J. Phys. Chem. B* **103** (1999) 2042.
31. P. He, M. Lefèvre, G. Faubert and J.P. Dodelet, *J. New. Mat. Electrochem. Systems* **2** (1999) 243.
32. G. Faubert, R. Côté, J.P. Dodelet, M. Lefèvre and P. Bertrand, *Electrochim. Acta* **44** (1999) 2589.
33. M. Lefèvre, J.P. Dodelet and P. Bertrand, *J. Phys. Chem. B* **104** (2000) 11238.
34. C. Gerthesen, H.O. Kneser and H. Vogel, 'Physik', 15th edn. (Springer, Heidelberg 1986).
35. S. Gottesfeld, I.D. Raistrick and S. Srinivasan, *J. Electrochem. Soc.* **134** (1987) 1455.
36. R.C. Weast (Ed.), 'CRC Handbook of Chemistry and Physics', 68th edn. (CRC Press, Boca Raton, FA, 1987).